CEBAF Program Advisory Committee Eight Cover Sheet

This proposal must be received by close of business on Thursday, April 14, 1994 at:

CEBAF
User Liaison Office, Mail Stop 12 B
12000 Jefferson Avenue
Newport News, VA 23606

Proposal Title

THE $\Delta(1232)$ FORM FACTOR AT HIGH MOMENTUM TRANSFER

Contact Person

Name: JIM NAPOLITANO
Institution: RENSSELAER
Address: DEPARTMENT OF PHYSICS
Address: RPI
City, State ZIP/Country: TROY NY 12180-3590
Phone: (518) 276-8019 **FAX:** (518) 276-6680
E-Mail Internet: JIMNAP@RPIHEP.PHYS.RPI.EDU

Experimental Hall: HALL C
Total Days Requested for Approval: 12.5
Minimum and Maximum Beam Energies (GeV): 4 GeV ONLY
Minimum and Maximum Beam Currents (μAmps): ≈ 100 μA

CEBAF Use Only

Receipt Date: 11/13/93 PR 94-114

By: [illegible]

HAZARD IDENTIFICATION CHECKLIST

CEBAF Experiment: PR 94-014 Date: May 24, 1994

Check all items for which there is an anticipated need—do not check items that are part of the CEBAF standard experiment (HRSE, HRSH, CLAS, HMS, SOS in standard configurations).

Cryogenics
- ____ beamline magnets
- ____ analysis magnets
- X target
- ____ drift chambers
- ____ other

Electrical Equipment
- ____ cryo/electrical devices
- ____ capacitor banks
- ____ high voltage
- ____ exposed equipment

Radioactive/Hazardous Materials
List any radioactive or hazadorous/ toxic materials planned for use:

Pressure Vessels
- ____ inside diameter
- ____ operating pressure
- ____ window material
- ____ window thickness

Flammable Gas or Liquids
(incl. target)
type: LIQUID HYDROGEN
flow rate: ____
capacity: ____
(Standard "4cm" Hall C Target)

Other Target Materials
- ___ Beryllium (Be)
- ___ Lithium (Li)
- ___ Mercury (Hg)
- ___ Lead (Pb)
- ___ Tungsten (W)
- ___ Uranium (U)
- ___ Other (list below)

Vacuum Vessels
- ____ inside diameter
- ____ operating pressure
- ____ window material
- ____ window thickness

Radioactive Sources
- ____ permanent installation
- ____ temporary use

type: ____
strength: ____

Large Mech. Structure/System
- ____ lifting devices
- ____ motion controllers
- ____ scaffolding or elevated platforms
- ____ other

Lasers
type: ____
wattage: ____
class: ____

Installation
- ____ permanent
- ____ temporary

Use
- ____ calibration
- ____ alignment

Hazardous Materials
- ___ cyanide plating materials
- ___ scintillation oil (from)
- ___ PCBs
- ___ methane
- ___ TMAE
- ___ TEA
- ___ photographic developers
- ___ other (list below)

Notes:
THIS EXPERIMENT USES ONLY THE STANDARD SET OF HMS (proton) AND SOS (electron) EQUIPMENT (INCL. TARGET)

Proposal to CEBAF PAC8:

The $\Delta(1232)$ Form Factor at High Momentum Transfer

J. Napolitano (co-spokesperson), P. Stoler (co-spokesperson)
G. Adams, M. Witkowski, B. Wojtsekhowski, N. Mukhopadhyay (theory)
Physics Dept., Rensselaer Polytechnic Institute, Troy NY 12180

V. Burkert, R. Carlini, Y. Chen, D. Mack, J. Mitchell, S. Wood
CEBAF, 12000 Jefferson Ave., Newport News, VA 23606

R. Minehart
University of Virginia, Univ. of Virginia, Charlottesville, VA 22903

E. Kinney, R.J. Peterson, R. Ristinen
Physics Dept., Univ. of Colorado, Boulder, CO 80309

E.W. Kim, C. Papanicolas, S. Williamson
Physics Dept., Univ. of Illinois, Urbana, IL 61801

Ts. Amatieni, G. Kazarian, H. Mkrtchyan
Yerevan Physical Institute, Armenia

April 13, 1994

Abstract

We propose to measure the transition amplitudes of the $\Delta(1232)$ resonance at $Q^2 = 4$ GeV^2/c^2. In particular we will measure the kinematically complete reaction $p(e,e'p)\pi^0$ at excitation energies covering the $\Delta(1232)$, obtaining nearly a full 4π angular distribution of the $p\pi^0$ in the Δ rest frame. This angular distribution depends strongly on the amplitude ratio E_{1+}/M_{1+} and the prediction of pQCD ($E_{1+}/M_{1+}= 1$) is very different from that of the constituent quark model ($E_{1+}/M_{1+}\approx 0$). Our momentum transfer is higher than any achieved in existing measurements. The experiment will be done in Hall C using the Short Orbit Spectrometer (SOS) to detect the scattered electrons, and the High Momentum Spectrometer (HMS) to detect the proton. Only single meson production is kinematically allowed at these energies, and the π^0 will be identified by missing mass. The experiment uses a 4 GeV, 100 μA beam, and a 4 cm liquid hydrogen target. There will be one setting of the electron spectrometer which defines Q^2. In order to cover the 4π decay of the Δ we need up to 4 angular settings of the proton spectrometer. The experiment will use only the initial complement of equipment in Hall C. Data collection time will be about 10 days. The total request including contingency is 300 hours.

1 Proposal Summary

This experiment will measure exclusive single π^0 production on protons in the excitation region of the $\Delta(1232)$ resonance at $Q^2 = 4\ GeV^2/c^2$. Our goal is to measure the angular distribution of $\Delta(1232) \rightarrow p\pi^0$ at the highest practical Q^2 at CEBAF. If a transition away from the simple CQM toward perturbative QCD (pQCD) begins to be effective at these energies, as suggested by by theory [Br89] and experiment [St91b, St93], then E_{1+}/M_{1+}should significantly increase (in the pQCD limit $E_{1+}/M_{1+} \approx 1$) which determines the angular distribution. On the other hand, the predictions of the constituent quark model (CQM), including aspects of QCD as well as relativistic effects [Ca92], are that $E_{1+}/M_{1+} \approx 0$, and the resulting angular distribution is markedly different. Existing data on this angular distribution at $Q^2 \approx 3\ GeV^2/c^2$ is inconclusive [Wa90], but allows for the possibility of a large E_{1+}/M_{1+}, in fact approaching unity. Systematic uncertainty will limit our sensitivity to E_{1+}/M_{1+}, but we expect to be sensitive to values down to ≈ 0.1.

The experiment will be carried out in Hall-C using the Short Orbit Spectrometer (SOS) to detect the scattered electrons, and the High Momentum Spectrometer (HMS) to detect the recoiling proton. The emitted π^0 will be identified by missing mass reconstruction.

The proposal and techniques described here were initially proposed by some members of the present collaboration to the PAC in 1988 , in conjunction with a proposal to construct a non-focussing spectrometer. At that time we pointed out that the detector configuration in Hall C would be highly suitable for studying resonances at high Q^2 via the reaction $p(e, e'p)\pi^0$, due to the kinematic focussing of the decay proton into a narrow cone, especially in the case of the $\Delta(1232)$. This is the basis of the present proposal.

We propose to study the short range structure of the Δ resonance in a kinematic region which has never before been studied by exclusive coincidence reactions using the same technique. A number of other experiments at CEBAF and other laboratories will study the $\Delta(1232)$. However, only experiment E-91-002 [St91a], which will use the CLAS, has as its primary motive the study of the high Q^2 evolution of the contributing amplitudes, while experiment E-89-037 [Bu89] concentrates at lower Q^2. The present proposal is complementary to the program at CEBAF to study the properties of resonances in general, and in particular the $\Delta(1232)$. It is complementary to the CLAS experiments in that the characteristics of the employed instruments are very different, each with its distinct advantages. CLAS is a very high acceptance device which will simultaneously accumulate a large body of data for many reactions over a very large kinematic region. However, its

acceptance is complicated, and its luminosity is limited. The HMS-SOS combination can handle high luminosities, has a simpler, more easily understood acceptance, but is limited to experiments with well focussed kinematics. The present experiment makes maximal use of these advantages and limitations. It is also complementary in that it will give us a well defined result with which the future CLAS experiments will calibrate.

2 Physics Background

One of the fundamental problems in physics concerns the structure of hadrons (mesons and baryons) and their excitations in terms of quark and gluon constituents. A central question concerns which models are valid for describing these excitations in different domains of Q^2. At low Q^2 ($< 1\ GeV^2/c^2$) in the non-perturbative QCD (NpQCD) domain, CQM's have been used to describe available data - sparse as they are. In the limit of very high Q^2 it is widely believed that pQCD descriptions would be appropriate. However, there is currently strong disagreement as to what domain of Q^2 corresponds to the transition from NpQCD to pQCD descriptions. Some [Br89, Ca88, Li92] believe the transition may take place for Q^2 as low as a few GeV^2/c^2 while others [Is89, Ra91] maintain that the transition should occur in a much higher region of Q^2. Recently, calculations taking into account color radiative "Sudakov" effects [Li92] support the former point of view.

During the past several years, proton elastic scattering form-factor data [Ar86, Ar93] have provided some of the primary data for testing these questions. This data provides strong evidence that CQM's cannot be applied for Q^2 above a few GeV^2/c^2. For example Figure 1 shows the result of a relativistically invariant CQM calculation of the proton magnetic form factor [Dz88] compared with the experimental data. Already at Q^2 = 2-3 GeV^2/c^2 the theory significantly underestimates the experimental results. However, the calculation utilized a Gaussian potential, which introduces large damping with Q^2, and recent calculations [Br94, Zh94] suggest that at Q^2 even beyond the Q^2 where CQM's are useful, soft processes can mimic pQCD predicted scaling behavior. This is the region in Q^2 which we would like to access in the present proposal.

The study of the properties of electromagnetic transitions to resonant excited states is also a very important area for testing models of baryon structure. This is reviewed in [St93]. Unfortunately not much is known for Q^2 greater than a few GeV^2/c^2. This is because the resonances are broad, strongly overlapping, with a significant underlay of non-resonant background. This is seen in single arm data of Figure 2. Although one observes

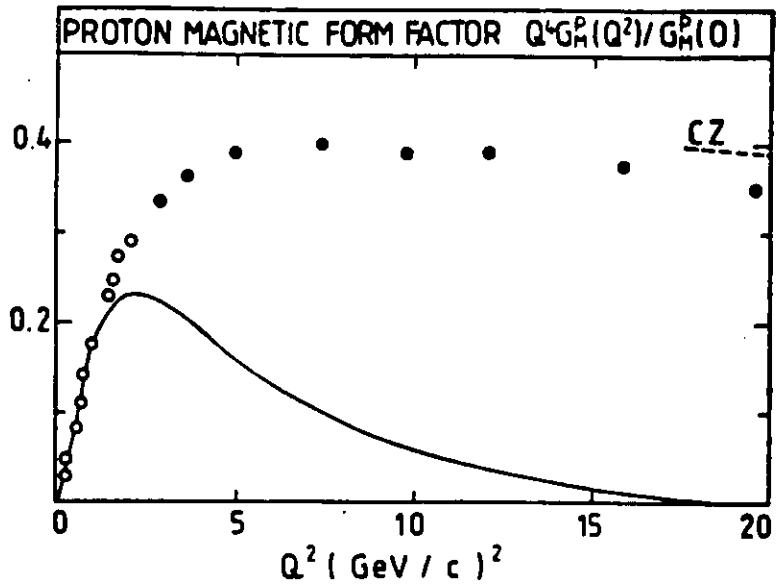

Figure 1: The proton elastic magnetic form factor G_M, calculation and experimental data.

three peaks, there are some 20 known light-quark resonances of mass less than 2 GeV.

2.1 Transition Multipoles

The way to get at the multipoles of the individual resonances is to perform coincidence experiments in which the angular dependences of the decay products are analyzed. In this regard the $\Delta(1232)$ is the most favorable case to study, since as seen in Figure 2, it is the only resonance which does not strongly overlap any of the others. Furthermore, its only strong decay is by single pion emission, and the level of underlying background can be strongly reduced by selecting the π^0 channel, since the normally dominant "seagull" and t-channel background terms are absent. From the physics point of view the $\Delta(1232)$ has the additionally attractive feature that $J = 3/2$, so that there are three contributing multipoles, E_{1+}, M_{1+}, and S_{1+} whose relative contributions are model dependent.

At low Q^2 in a pure $SU(6)$ non-relativistic CQM, the $N \rightarrow \Delta$ transition is purely M_{1+} in character, involving a single-quark spin-flip with $\Delta L = 0$. An E_{1+} contribution is not permitted since the Δ and N are both in $L = 0$ states which cannot be connected by an operator involving $L > 0$. The addition of a residual quark-quark color magnetic interaction adds higher L components to the Δ wave function, and thus introduces a small E_{1+} component of perhaps a few percent. The measurement of this small E_{1+}/M_{1+} ratio is one of the most interesting problems in baryon resonance physics in that it will give very powerful tests of the CQM in the low Q^2 regime. At $Q^2 = 0$ the experimental data supports

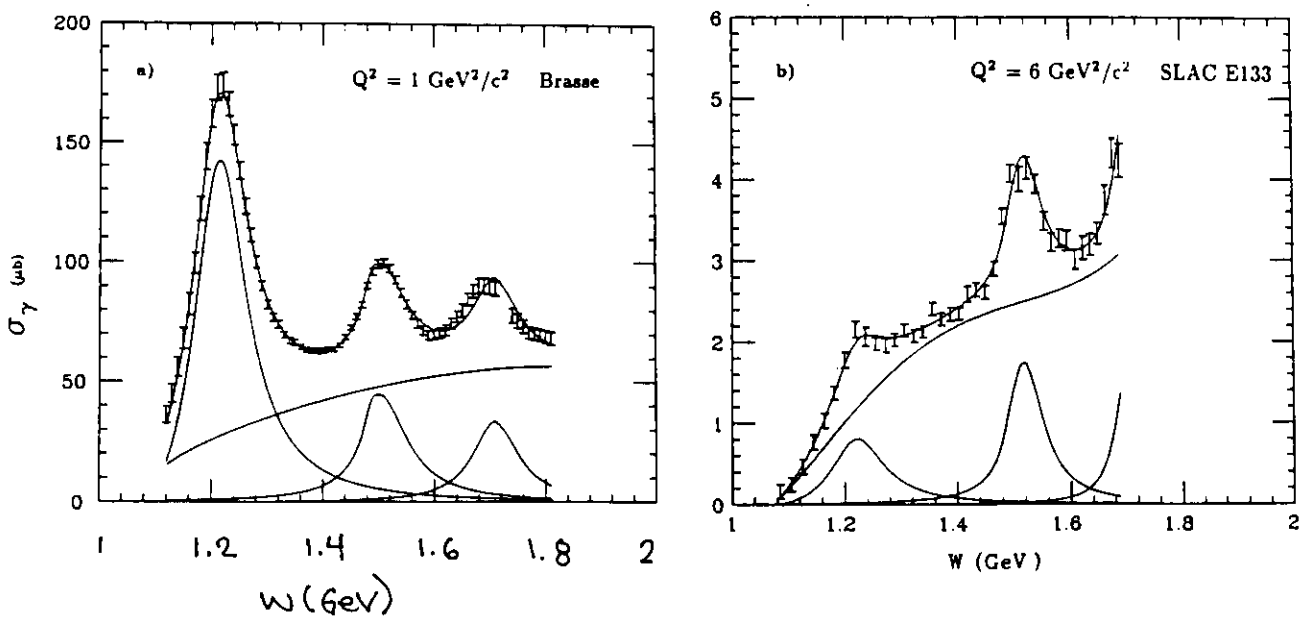

Figure 2: The virtual photon excitation curves for electron scattering at $Q^2 = 1$ and 6 GeV^2/c^2.

the CQM prediction of M_{1+} dominance extremely well. A review by [Da90, Da91] finds

$$M_{1+} = 285 \pm 37 \times 10^{-3} GeV^{-1}$$
$$E_{1+} = -4.6 \pm 2.6 \times 10^{-3} GeV^{-1}$$

or $|E_{1+}/M_{1+}| = 0.016 \pm 0.009$. As Q^2 increases there is no reason to expect the E_{1+}/M_{1+} ratio to remain extremely small. For $Q^2 > 0$ the experimental situation is shown in Figure 3 as summarized by [BuPC]. Nearly all the available data is for $Q^2 < 1\ GeV^2/c^2$. The fact that $Re(E_{1+}^* M_{1+})/|M_{1+}|^2$ (for which we write E_{1+}/M_{1+}) remains very small is further evidence that the CQM continues to work well for low Q^2. The one experimental point at $Q^2 = 3\ GeV^2/c^2$ ($E_{1+}/M_{1+} = 0.08 \pm 0.06$) is statistically not significant enough to make any conclusions, although it is suggestive. In any case, this was extracted by fitting data under the assumption that E_{1+}/M_{1+} is very small so that various multipole contributions in the data are neglected. However, [Wa90] have pointed out that one can obtain an equally consistent fit to the data on which the analysis is based by assuming that $E_{1+}/M_{1+} \sim 1$ so we must conclude that the magnitude of E_{1+}/M_{1+} at $Q^2 = 3\ GeV^2/c^2$ is unknown.

What does one expect above $Q^2 \sim 2\ GeV^2/c^2$? At this point, beyond the CQM based calculations there is no theoretical guidance. In fact, one of the most rigorous CQM

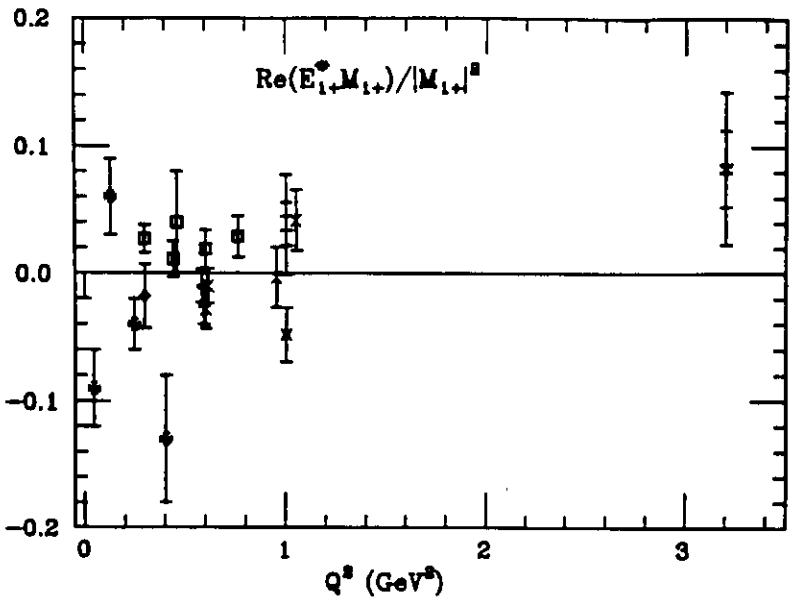

Figure 3: Evaluation of $Re(E_{1+}^* M_{1+})/|M_{1+}|^2$ from available data.

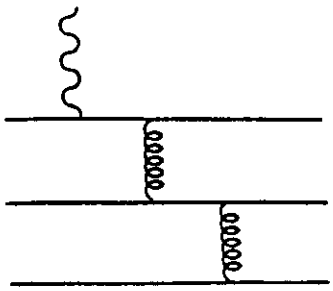

Figure 4: Typical leading order diagram contributing to a baryon form factor at high Q^2.

calculations [Ca92] obtains a very small E_{1+}/M_{1+} even up to Q^2>3 GeV^2/c^2. However, there is a theory which relates to high Q^2. It is believed that all exclusive reactions should proceed by leading order processes involving Fock states having the minimum number of current quarks (ie. the valence quark configuration) which exchange the minimum number of gluons. For a baryon, the transition amplitude is obtained by evaluation of diagrams such as shown in Figure 4. Such processes could in principle be evaluated perturbatively, since all momentum transfers between quarks and gluons are large.

A further constraint is that of helicity conservation at the vertices of the quarks with the vector fields, ie. photons and gluons. For electromagnetic processes involving cylindrical symmetry this implies that the overall helicity of the baryon is conserved. Thus helicity non-conserving amplitudes are expected to vanish relative to helicity conserving amplitudes

at the high Q^2 limit.

The multipoles may be expressed in terms of helicity conserving and non-conserving amplitudes as follows:

$$\begin{aligned}
\Delta\lambda = 0 \quad &\Rightarrow \quad A_{1+} = \frac{3}{2}M_{1+} + \frac{1}{2}E_{1+} \\
\Delta\lambda = 2 \quad &\Rightarrow \quad B_{1+} = E_{1+} - M_{1+} \\
\Delta\lambda = 1 \quad &\Rightarrow \quad C_{1+} = \frac{2Q^2}{p_\pi^*}S_{1+}
\end{aligned}$$

Thus, helicity conservation implies $B_{1+} = 0$, or $E_{1+}/M_{1+} = 1$, quite different from low Q^2. In the present experimental situation, we do not expect to have reached the perturbative regime, however we may expect to observe a significant increase in E_{1+}/M_{1+}. Recently [Li92] has shown that color radiative corrections (Sudakov effects) reduce the non-leading contributions to elastic form-factors (which dominate the CQM approach) relative to the leading contributions (which dominate the pQCD approach) so that the transition from CQM to pQCD occurs at lower values of Q^2 than might otherwise be expected. One may speculate that this may be the underlying reason why so many exclusive reactions appear to obey the simple Q^2 counting rules at unexpectedly low values of Q^2. (However, see [Br94, Zh94].)

2.2 Form Factors

The current experimental situation, summarized in Figure 3, is that there exists no exclusive data above 3 GeV^2/c^2, and the data at 3 GeV^2/c^2 are quite sparse. Existing single-arm inclusive electron scattering data have been evaluated [St91b], and form-factors extracted for the peaks corresponding to the first, second and third resonance regions. Transverse resonance form-factors G_T are defined [Ca88] in analogy with elastic scattering form-factors:

$$\frac{d\sigma}{d\Omega dE} = \Gamma\sigma(W_R) \quad \text{with} \quad \sigma(W_R) = \frac{8\pi\alpha Q^2 M_N}{W_R K_R}G_T^2$$

where $\sigma(W_R)$ is the virtual photon cross section at the resonance energy W_R, K_R is the equivalent real photon energy at W_R, and the quantity Γ is the virtual photon flux factor (see Appendix).

The evaluation of the leading order transition amplitudes for exclusive processes using pQCD leads to Q^2 scaling laws, which remarkably appear to be obeyed even at relatively low Q^2. For example, evaluation of diagrams such as in Figure 4 leads to a Q^{-4} behavior for

helicity conserving form factors, and a greater fall off with Q^2 for helicity non-conserving form factors, eg Q^{-6} for $\Delta\lambda$=2. There is also a logarithmic decrease due to the Q^2 dependence of the running coupling constant α_s, but this would be observable only over a large range of Q^2.

Transition form-factors G_T for the $\Delta(1232)$ and the peaks near W=1535 and 1680 MeV, as a function of Q^2 were obtained by fitting Breit-Wigner resonance shapes together with phenomenological backgrounds to existing inclusive data, such as in Figure 2. These are shown in Figure 5 relative to a dipole shape $G(Q^2)_{dipole} = 3/(1 + Q^2/0.71)^2$. Included in Figure 5 is the proton elastic form-factor. Also shown at lower Q^2 are form-factors extracted from data obtained from exclusive $(e, e', p)\pi^0$ and $(e, e', p)\eta$ experiments [Ha79, Fo83, BuPC].

In Figure 5 the ratio $G_M(Q^2)/G(Q^2)_{dipole}$ is plotted rather than $Q^4 G_M(Q^2)$ to better display the low Q^2 behavior. For high Q^2 the quantity $Q^4 G(Q^2)_{dipole} \rightarrow constant$. In fact the elastic form-factor G_M does appear to approach this behavior above $Q^2 \sim 5\ GeV^2/c^2$ out to the highest measured Q^2 ($\sim 35\ GeV^2/c^2$). This Q^2 behavior as well as the magnitude (see below) has been one of the key elements in support of the proponents of pQCD at experimentally accessible values of Q^2. The second and third resonance transition form-factors also appear to approach the predicted Q^{-4} behavior, within quite large statistical errors.

The $\Delta(1232)$ form-factor decreases faster than Q^{-4} at all observed Q^2, that is at low Q^2 where CQM's are expected to work well, as well as at higher Q^2 where CQM are not appropriate. The reason for this anomalous behavior is not currently understood, however it has been suggested [Ca88] that this may be due to the suppression of the leading order pQCD amplitude, and the dominance of higher order amplitudes in regions of Q^2 where leading order contributions are already important in other form factors.

3 Experimental Considerations

3.1 Acceptances

It is proposed to measure the reaction $p(e, e'p)\pi^0$ using the SOS spectrometer to detect the scattered electrons and the HMS spectrometer to measure the recoil protons. Due to a large kinematic boost at this high Q^2 the hadrons are always emitted in a narrow forward

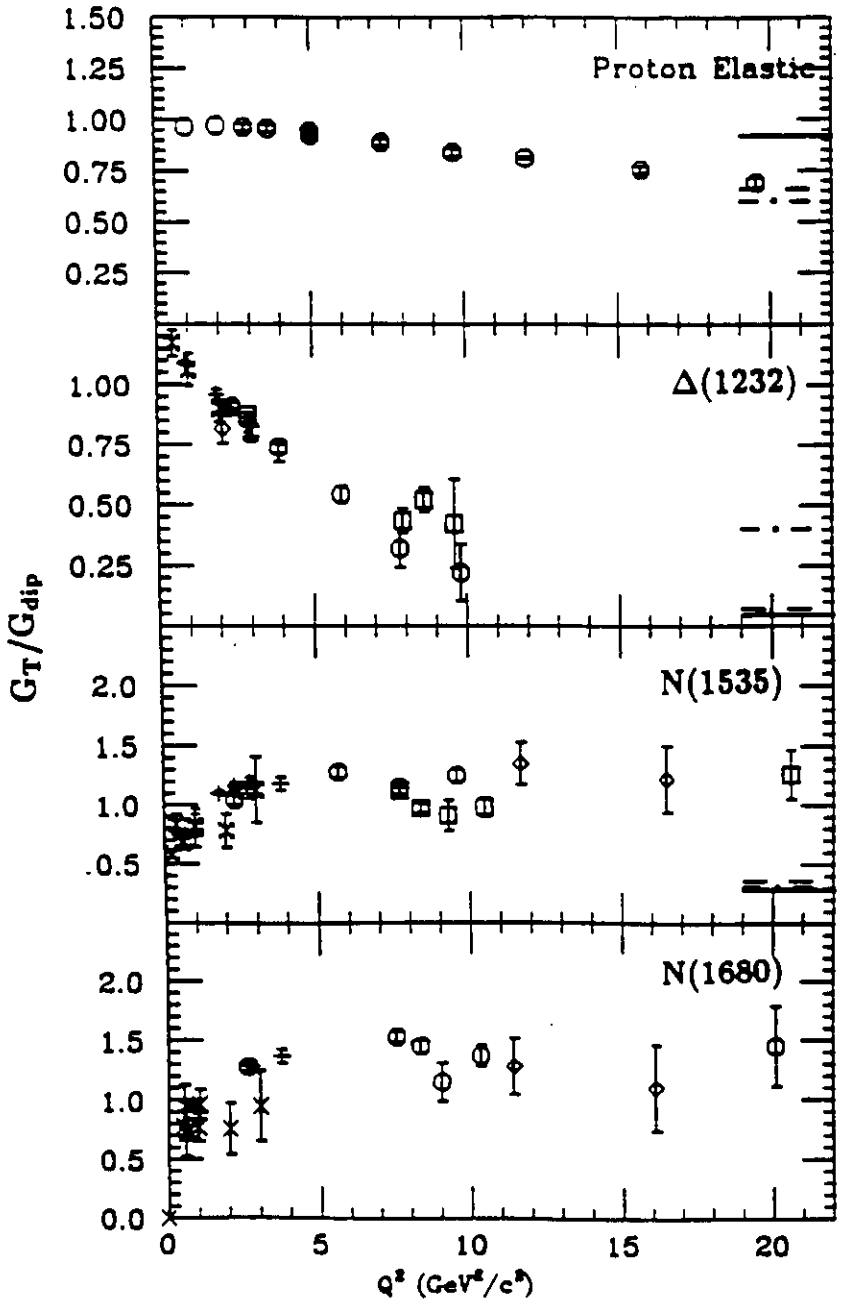

Figure 5: (a) The transverse magnetic form- factor divided by the dipole shape G_M/G_{dipole} versus Q^2 for elastic scattering from the proton, and for inelastic excitation of the $\Delta(1232)$, $S_{11}(1535)$, and $F_{15}(1680)$ resonance regions. The resonance form-factor G_T and the dipole form factor G_{dipole} are defined in the text.

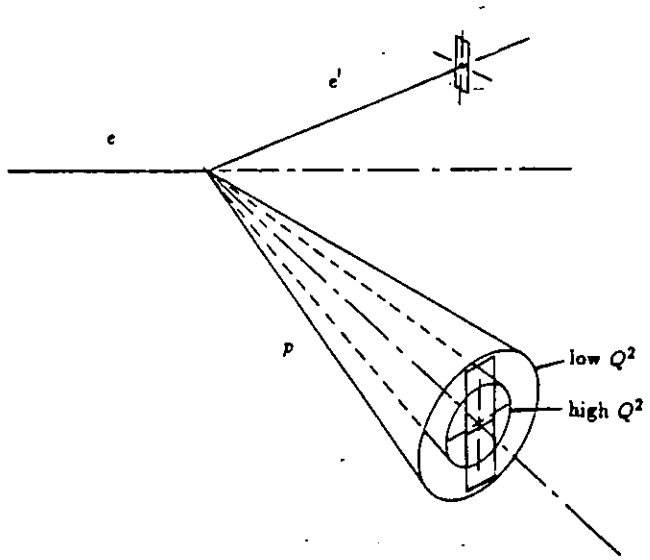

Figure 6: Illustration of the envelope of the proton laboratory angle relative to the momentum transfer vector.

cone about the momentum transfer direction. This is illustrated in Figure 6.

Thus one sees that by detecting the proton it is possible to measure a 4π angular distribution with a moderate solid angle spectrometer. Also shown in Figure 6 is the vertical acceptance of the HMS. However, the horizontal acceptance of the HMS is rather narrow so that 4 horizontal angular settings will be required to cover the full solid angle (Figure 7). Likewise, the momentum acceptance of the HMS is not great enough to cover the full range of proton momenta at a given angular setting, so that two and three will be necessary at each pair of angular settings. We estimate that we would require a total of about 10 angle-central momentum settings.

Figure 8 shows the cm decay angle and proton momentum coverage for each setting of the HMS spectrometer for an electron kinematics fixed at the center of the SOS acceptance. The finite acceptance of the SOS will broaden the acceptances shown in the figure.

3.2 Backgrounds

One of the major sources of background will be energetic pions misidentified as electrons. Using the EPC code of Lightbody and O'Connell [Li88], and the known inclusive electron cross sections for the present kinematics we find the ratio of negative pions to true electrons is calculated to be about 3 to 1. These will be eliminated by the SOS gas Cerenkov counter.

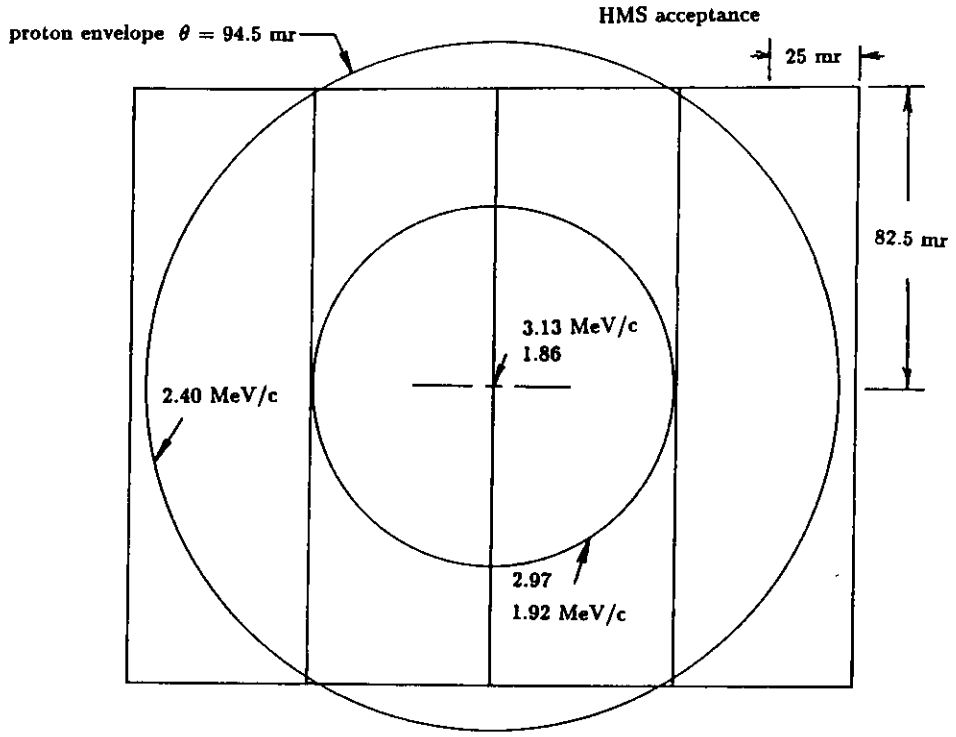

Figure 7: The acceptance of the HMS spectrometer for an electron kinematics fixed at the center of the SOS acceptance. The finite acceptance of the SOS will broaden the acceptances shown in the figure. The outer circle is the envelope of the maximum lab. angle of the cone corresponding to a full 4π cm decay.

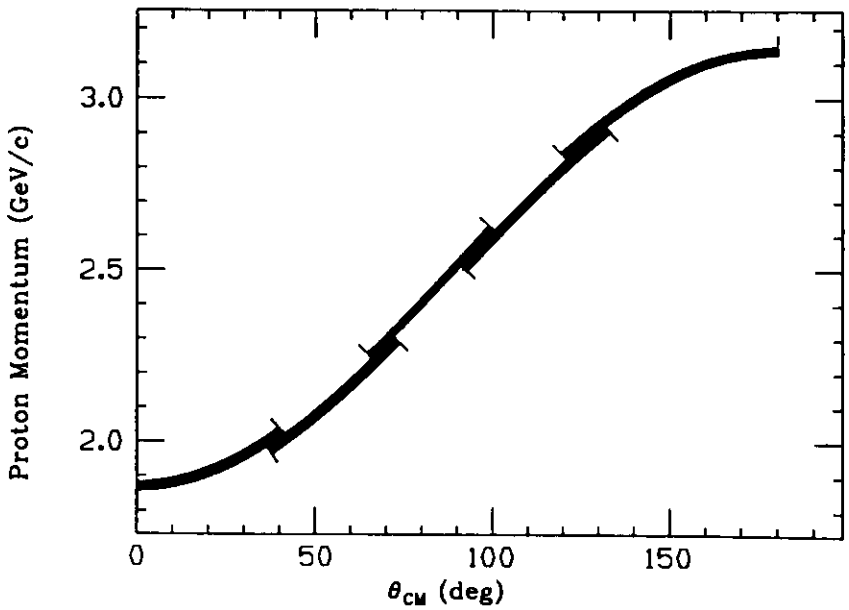

Figure 8: The acceptance of the HMS spectrometer in delta cm decay angle and proton momentum for the HMS lab angular settings shown in Figure 7. The finite acceptance of the SOS will significantly broaden and overlap the acceptances shown in the figure.

Table 1: Relative Accidental Rates

$\theta_p(deg)$	$P_0(GeV/c)$	$\Delta P(GeV/c)$	N_{acc}/N_{true}
22.27	1.89	.28	5×10^{-4}
22.27	3.05	.46	3×10^{-6}
25.14	2.18	.32	1×10^{-4}
25.14	2.44	.36	3×10^{-5}
25.14	2.80	.41	4×10^{-5}

Accidental coincidence background rates were also estimated with the aid of the EPC code [Li88], for the proposed running conditions and experimental setup. The results are tabulated in Table 1.

3.3 Missing Mass Resolution

Any remaining background will be eliminated using several techniques, including coincidence timing, trajectory traceback to the target, and most importantly by requiring the missing mass constraint

$$M_X^2 \equiv (p_e + p_p - p_e' - p_p')^2 = m_\pi^2$$

be satisfied. The missing mass technique for π^0 and η electroproduction has been successfully used previously with magnetic spectrometers, eg. at DESY [Br84]. We will be in a more favorable situation than earlier work for several reasons. First, we are working at an excitation energy where only one pion can be emitted, so that there will be no real multipion continuum. Furthermore, the resolution of the SOS-HMS combination is much better than in other measurements, eg [Br84], so that we will obtain a much narrower and higher π^0 peak.

We have simulated the missing mass resolution, using predicted resolutions in angle and momentum for the HMS and SOS. In particular, we used the RMS resolutions $\delta p/p = 5.9 \times 10^{-4}$, $\delta\theta = .54$ mr, and $\delta\phi = .65$ mr for the HMS, and $\delta p/p = 1 \times 10^{-3}$, $\delta\theta = 1.0$ mr, and $\delta\phi = 1.0$ mr for the SOS. The result is shown in Figure 9. The π^0 peak is well separated from the position of the elastic peak and the minimum 2π mass. Furthermore, the software cuts in the electron spectrometer excitation spectra will eliminate the elastic peak, and will be almost completely below the 2π threshold.

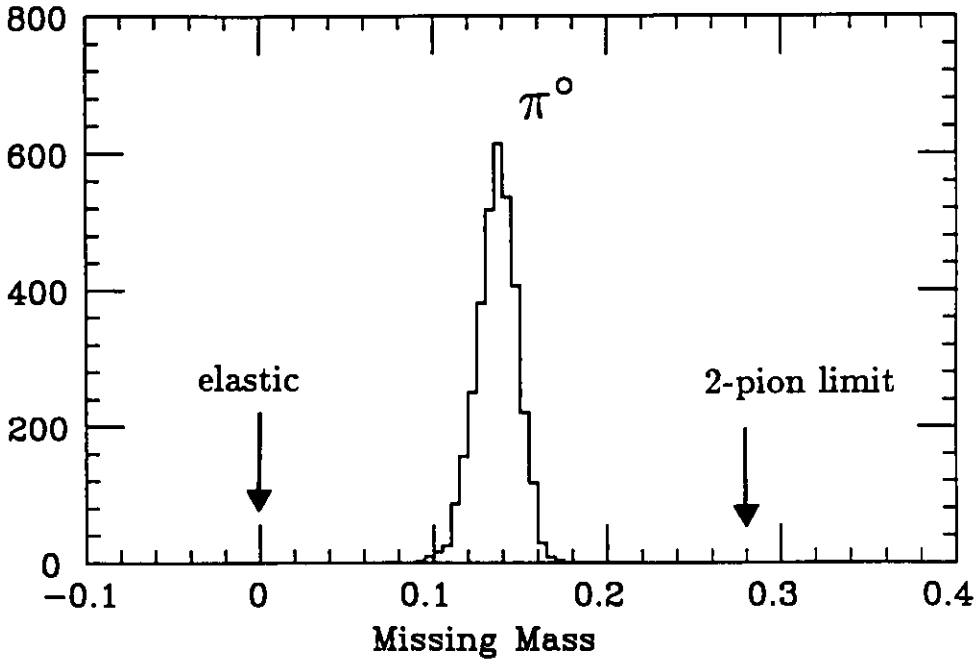

Figure 9: The missing mass spectrum in $p(e,e'p)\pi^0$.

4 Multipoles and Angular Distributions

With unpolarized beam and target the differential cross section as a function of pion angles (θ,ϕ) relative to the direction of the virtual photon may be expressed as

$$\frac{d\sigma}{d\Omega_\pi} = F\left[A(\theta) + \epsilon B(\theta) + \epsilon C(\theta)\cos(2\phi)\sin^2\theta + \sqrt{\epsilon(\epsilon+1)}D(\theta)\cos\phi\sin\theta\right] \qquad (1)$$

In the above

$$F \equiv \frac{|\vec{p}_\pi|W}{MK} \quad \text{with} \quad K = \frac{W^2 - M^2}{2M}$$

In general, each resonance is characterized by three complex multipoles M_J, E_J, and S_J. In the case of the $\Delta(1232)$ we have $J = l + 1/2 \equiv l+$, with $l+ = 1+$. In the region of the $\Delta(1232)$ the non-resonant Born terms are relatively significant, but are rather well understood. In any case, the selection of the π^0 channel strongly suppresses the relative Born contributions in comparison with their contribution to the inclusive cross section. There are also relatively small contributions due to the tails of higher resonances which need to be included in the analysis of the measured cross sections.

In the this experiment the angular distribution will be very sensitive to the relative contributions of the E_{1+} and M_{1+} multipoles, even if $E_{1+} << M_{1+}$. This is seen as follows: The expression of the coefficients in eq.1 above in terms of multipoles is given in the Appendix. To simplify the explanation we retain only M_{1+} and E_{1+}, and we neglect multipoles of order $|E_{1+}|^2$. Under these conditions the only remaining coefficients in eq. 1

are A and C, which may be written

$$\begin{aligned} A &= A_0 + A_2 \cos^2(\theta) \quad \text{with} \\ A_0 &= \frac{5}{2}|M_{1+}|^2 - 3Re(M_{1+}E_{1+}^*) \\ A_2 &= -\frac{3}{2}|M_{1+}|^2 + 9Re(M_{1+}E_{1+}^*) \quad \text{and} \\ C &= C_0 = -\frac{3}{2}|M_{1+}|^2 - 3Re(M_{1+}E_{1+}^*) \end{aligned} \tag{2}$$

The factor of 9 in the expression for A_2 results in a very large angular sensitivity to $Re(M_{1+}E_{1+}^*)$.

Differential cross sections were calculated at Q^2=4 GeV^2/c^2 assuming E_{1+}/M_{1+}=0, 0.1, and 0.2. The calculations use the *full* expression, without any assumptions about the magnitude of E_{1+}/M_{1+}, but with the assumptions $S_{1+} = 0$, and that the phases of E_{1+} and M_{1+} are equal. The calculations also include the non-resonant Born amplitudes up to a partial wave $L = 5$. The multipole amplitudes for all cases were normalized to yield the same angle integrated resonance cross section $\sigma(W_R) = 3.3\mu b$ as estimated from [St91b]. These amplitudes are those shown in Table 2 in Section 5 of this proposal.

Angular distributions in θ for three values of fixed ϕ are shown in Figure 10.

One observes that there is a great deal of sensitivity to the ratio E_{1+}/M_{1+} over much of the $(\cos\theta, \phi)$ kinematic plane, whereas the lack of sensitivity at other regions will serve as an important constraint on the overall analysis. Also shown in Figure 10 is the non-resonant Born contribution, which is seen to be rather small. Other backgrounds, such as tails of higher resonances, will also contribute. One of the goals of our theoretical effort will be to characterize this background. The relative contribution of the background terms will be further reduced by selecting only $l = 1$ partial waves in the analysis. An important handle on the non-resonant contributions will be obtained by analysis of the data away from the central resonance energy. Figure 11 shows the angular distribution in θ for the same values of ϕ as in Figure 9, but off-resonance with baryon mass $W = W_R + 100$ MeV=1323 MeV. Here the non-resonant terms are comparable to the resonant terms giving rise to strong interference effects.

Asymmetries inherent in the cross sections of Figures 10 and 11 are very sensitive, to E_{1+}/M_{1+}. For example, Figure 12 shows the ϕ dependence of the asymmetry

$$\Sigma(\phi)_{(90-0)} \equiv \frac{\sigma(\theta = 90°) - \sigma(\theta = 0°)}{\sigma(\theta = 0°)}$$

at $W = W_R$ and $W = W_R + 100$ MeV. Figure 13 show the asymmetries

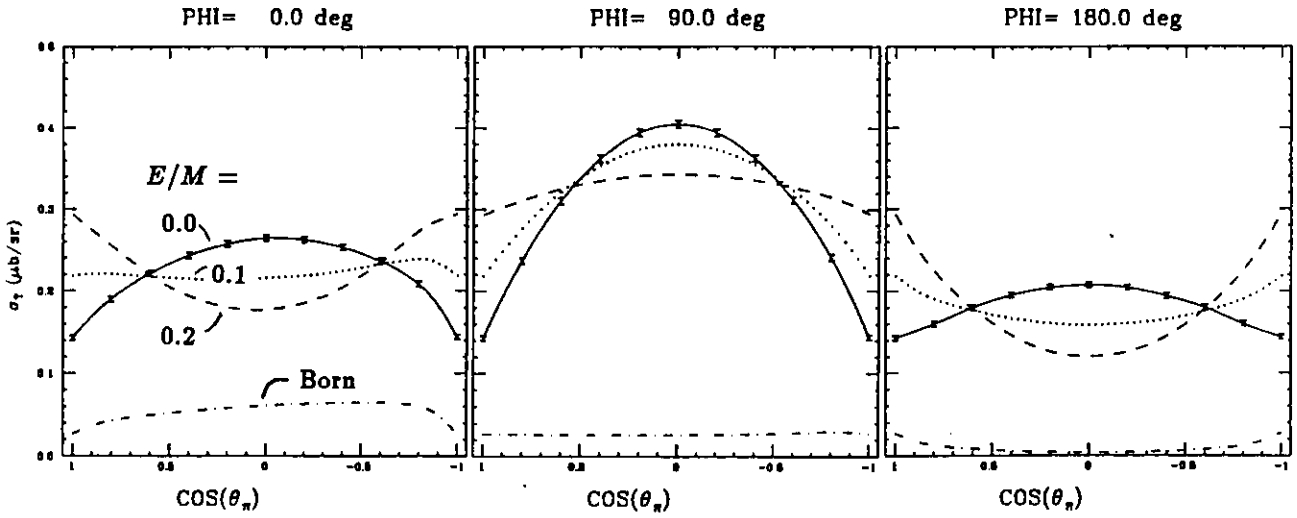

Figure 10: Calculated differential cross sections vs θ_{cm} of the detected proton at fixed values of ϕ_{cm} for the reaction $p(e,e'p)\pi^0$ at Q^2=4 GeV^2/c^2 , at $W = W_R = 1232$ MeV, including Born amplitudes, assuming a total resonance inclusive virtual cross section $\sigma = 3.3\mu b$. The three curves in each figure correspond to E_{1+}/M_{1+}=0.0, 0.1, and 0.2 respectively. The dotted points are the calculated non-resonant Born terms obtained by setting the resonant amplitudes to zero. The points with error bars are the expected statistics of the proposed experiments, under the data binning conditions discussed in the text. There will actually be a total of 9 such distributions in the experiment.

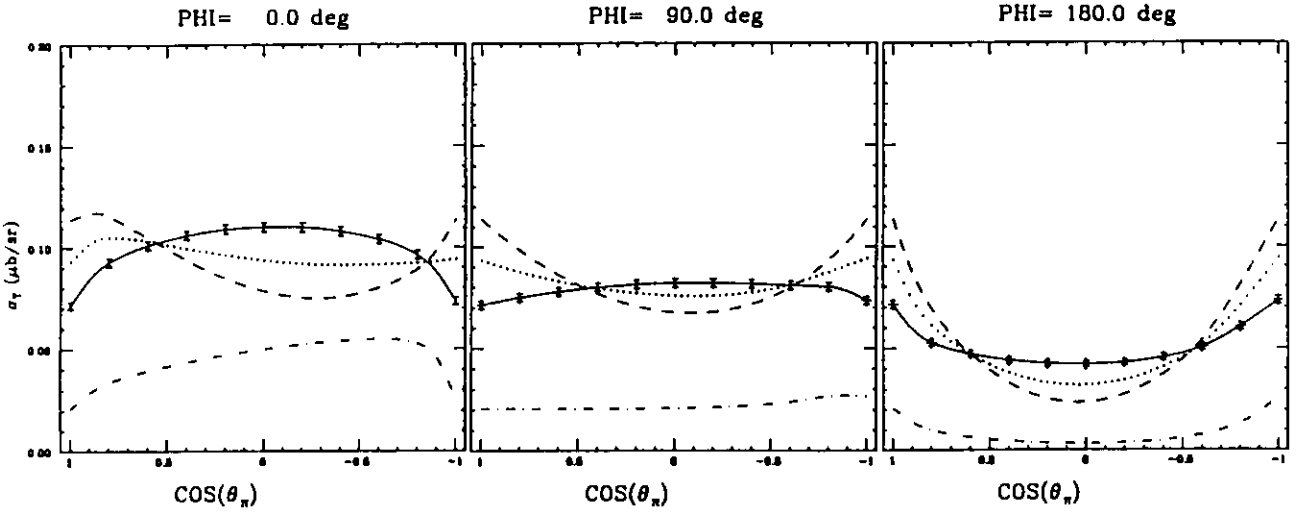

Figure 11: Same as in Figure 10, but at $W = W_R + 100$ MeV.

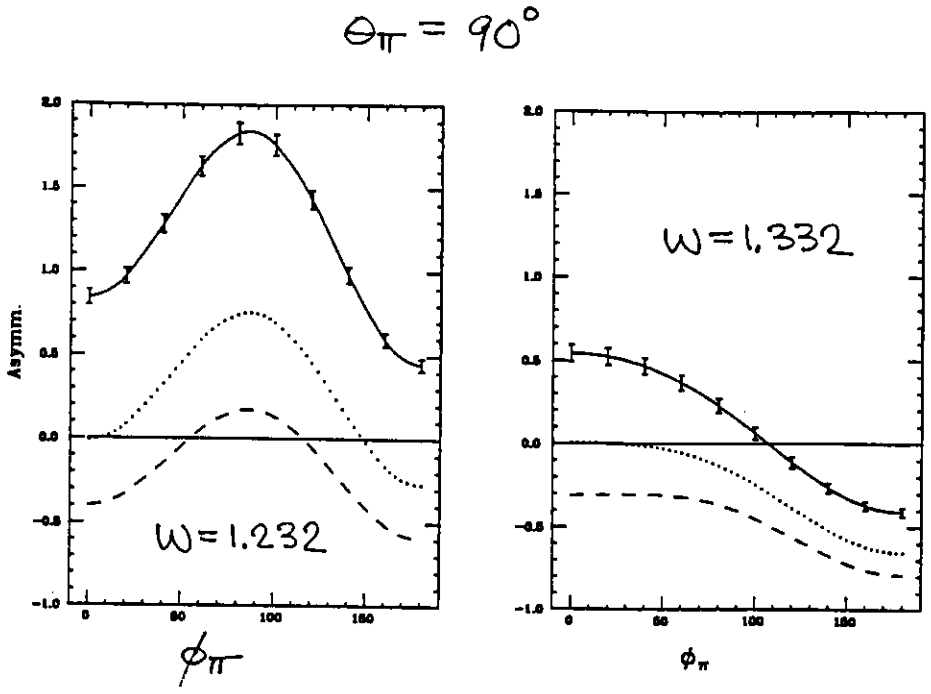

Figure 12: The calculated ϕ dependence of the asymmetry $\Sigma(\phi)_{(90-0)}$ at $W = 1232$ and 1323 MeV. The curves have the same meaning as in Figure 10.

$$\Sigma(\theta)_{(\theta-0)} \equiv \frac{\sigma(\theta) - \sigma(\theta = 0°)}{\sigma(\theta = 0°)}$$

for three fixed values of ϕ, on resonance at $W = 1232$ MeV and off-resonance at $W = 1332$ MeV.

One sees that the asymmetries are extremely sensitive to the assumed values of E_{1+}/M_{1+}. Note that in Figures 12 and 13 off resonance at $W = 1323$ MeV the interference between resonant and non resonant terms are now very important, leading to remarkable effects in the relative signs of the asymmetries as a function $\cos\theta$ depending on the fixed value of ϕ.

5 Statistical Accuracy of the Data

Estimates for the expected statistical accuracy of the data were carried out on the basis of assumptions shown in Table 2. The total number of events expected over a 10 day collection period for $W = 1232 \pm 50$ MeV over 4π (in the Δ center of mass frame) is about $\frac{1}{2} \times 10^6$, with lesser amounts as we go off resonance. In Figures 10 through 13 are plotted the expected statistical accuracy of the differential cross sections. Each point represents the data binned over the interval $\Delta \cos\theta = 0.2$, and $\Delta\phi = 40°$. The statistical relative standard deviation for one data point is typically $\frac{1}{2}\%$ on resonance and about 1% for the

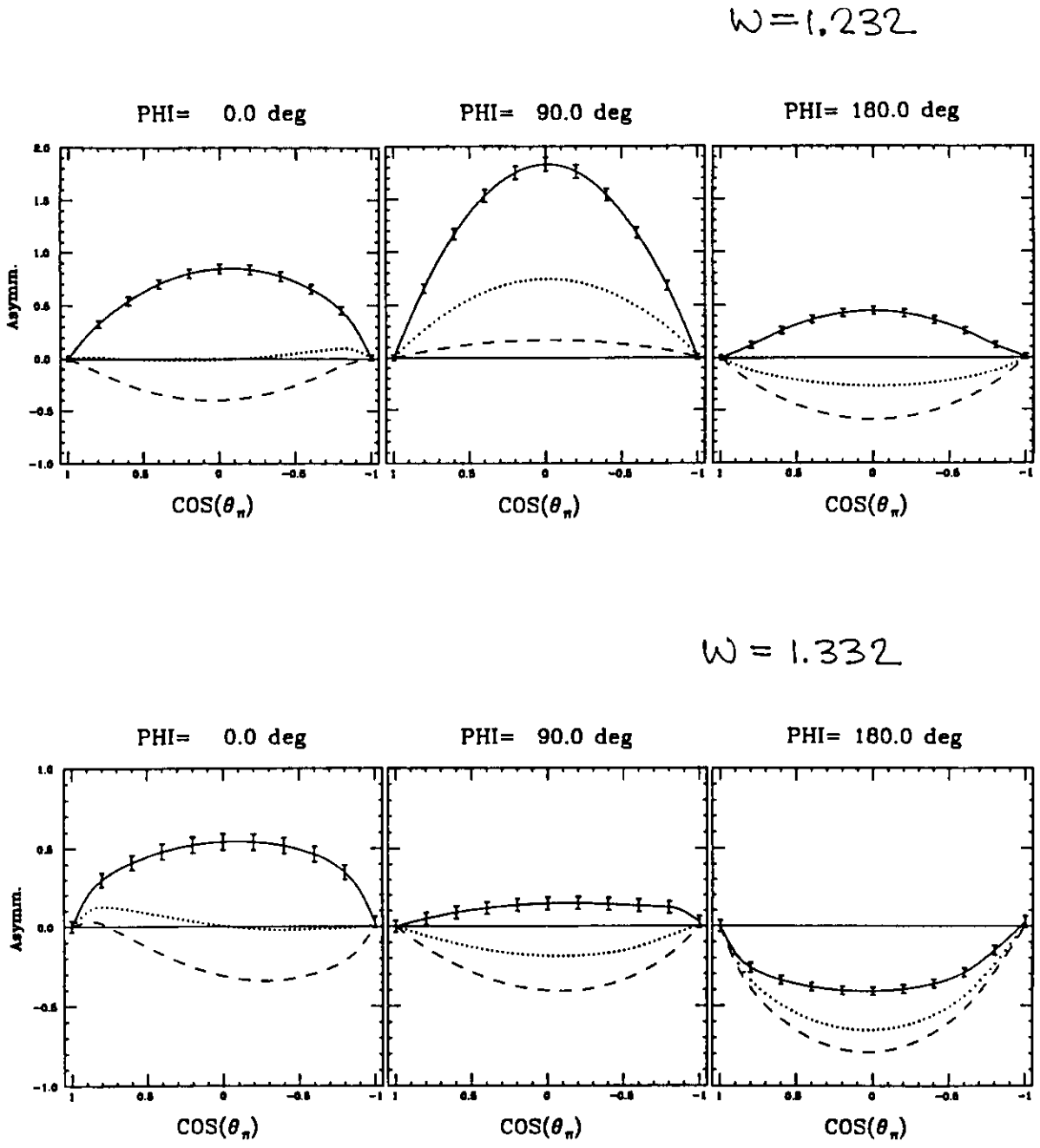

Figure 13: The asymmetries $\Sigma(\theta)_{(\theta-0)}$ for different fixed values of ϕ, on resonance at W = 1232 MeV and at W = 1332 MeV. The curves have the same meaning as in Figure 10.

Table 2: The kinematic conditions and acceptances used in estimating the statistics which would be expected for the experiment.

- Cross section $\sigma(W_R) = 3.3\mu$b
- Three combinations of amplitudes:
  - E_{1+}/M_{1+}=0.0 with $M_{1+} = -0.362\ \mu\text{b}^{1/2}$
  - E_{1+}/M_{1+}=0.1 with $M_{1+} = -0.357\ \mu\text{b}^{1/2}$ and $E_{1+} = -0.036\ \mu\text{b}^{1/2}$
  - E_{1+}/M_{1+}=0.2 with $M_{1+} = -0.343\ \mu\text{b}^{1/2}$ and $E_{1+} = -0.069\ \mu\text{b}^{1/2}$
- Electron arm (SOS):
  - $\theta_e = 48°$
  - $P_e = 1.53$ GeV/c
  - Solid angle $\Delta\Omega = 5$ msr
  - ΔW selected = 100 MeV
- Proton arm (HMS):
  - $\theta_q = 21°$
  - $P_{max} = 3.1$ GeV/c and $P_{min} = 1.8$ GeV/c
  - $\Delta x'\ (out - of - plane) = 165$ mrad
  - $\Delta y'\ (in - plane) = 50$ mrad
  - $\Delta P/P = 0.10$
  - Total number of angle and momentum settings = 8
- Time of data collection = 10 days (240 hrs)
- Luminosity $1 \times 10^{38}/\text{cm}^2\text{s}$ ($I = 100\ \mu$A, X_{target}=4 cm)
- Total number of events over $\Omega = 4\pi$ (within $W = 1232 \pm 50$ MeV)$\sim \frac{1}{2} \times 10^6$

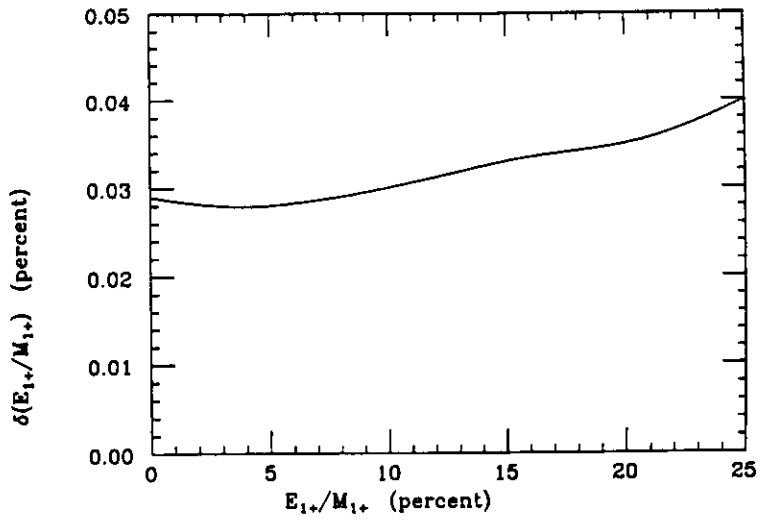

Figure 14: Projected Statistical Uncertainty in E_{1+}/M_{1+}.

adjacent off resonance intervals. There will be about 100 such data points over 4π for each W interval. The statistical uncertainties on the asymmetries are also very small, typically between 1 and 2%.

The estimated RMS statistical error in E_{1+}/M_{1+}, i.e. $\delta(E_{1+}/M_{1+})$, corresponding to the assumptions in Table 2 is shown in Figure 14. This error is extremely small, leading to the conclusion that the uncertainty will be dominated by systematics, and uncertainties in the underlying background multipoles and tails of higher lying resonances. Fortunately, in π^0 electroproduction the non resonant background is relatively small in the region of the $\Delta(1232)$, and the resonance is enough isolated from higher resonances so that their tails do not contribute strongly.

6 Systematic Errors

A very important control for this experiment is that at several kinematic settings of the proton detector we simultaneously collect data on the elastic channel $p(e, e'p)$. Since these cross sections are well known at the Q^2 of this experiment, this will serve as a very accurate normalization for our data. That is, it will pin down the product $N_e X_{target} \Delta\Omega_e \Delta\Omega_p$. Furthermore, the electron spectrometer (SOS) will always be run at the same angle and momentum settings so that by accumulating pre- scaled singles we will automatically get an accurate relative normalization for the runs involving different proton spectrometer

(HMS) settings. This will be extremely useful when the data are combined. Thus, in a sense the experiment will be self normalizing. In obtaining the asymmetries $\Sigma(\theta)$ or $\Sigma(\phi)$ the normalization factors cancel so that the systematic uncertainties would be even smaller.

References

[Ar86] R.G. Arnold et al., Phys. Rev. Lett., **57**, (1986) 174

[Ar93] T.A. Armstrong et al., Phys. Rev. Lett., **70** (1993) 1212

[Bl71] E. Bloom and F.J. Gilman, Phys. Rev., **D4** (1971) 2901

[Br84] F. W. Brasse et al., Z. Phys. **C22** (1984) 33;
F. W. Brasse et al., Nuc. Phys.**B139**(1978) 37

[Br94] V. I. Braun and I. Halperin, Phys.Lett. B, to be published

[Br89] S.J. Brodsky, Lectures at the 27th International School of Subnuclear Physics, Ettore Majorana Center for Scientific Culture, Erice (1989),SLAC-PUB-5116, and references therein; and P.Stoler,eds.,World Scientific, Singapore (1989), p122

[Bu89] V. Burkert, R. Minehart, et al. CEBAF Experiment E-89-037, "Electroproduction of the P33(1232) Resonance"

[BuPC] V. Burkert, private communication

[Ca92] Simon Capstick, Phys.Rev.D. **46** (1992)2864;
Simon Capstick and Nathan Isgur, Phys.Rev.D **34** (1986)2809

[Ca88] C.E. Carlson and J.L. Poor, Phys. Rev. **D38** (1988) 2758

[Ch84] V.L. Chernyak and A.R. Zhitnitsky, Phys. Rep. **112** (1984) 73

[Da90] R.M. Davidson and N.C. Mukhopadhyay, Phys. Rev. **D42** (1990) 20

[Da91] R.M. Davidson, N.C. Mukhopadhyay, and R. Whittman, Phys. Rev. **D43**(1991) 71

[Do78] A. Donnachie, G. Shaw, and D.H. Lyth in 'Electromagnetic Interactions of Hadrons', A. Donnachie and G. Shaw, eds., Plenum, New York (1978)

[Dz88] Z. Dziembowski, Phys. Rev., **D37** (1988) 778

[Fo83] F. Foster and G. Hughes, Rep. Prog. Phys. **46** (1983) 1445

[Ga86] M. Gari and N.G. Stephanis, Phys. Lett. **B175**(1986) 462;
M. Gari and W. Krupelmann, Phys. Lett. **B173**(1986)10

[Ha79] R. Haiden, DESY rep. F71-79/03

[Is89] N. Isgur and C.H. Llewellyn-Smith, Phys. Lett. **217B**(1989)535

[Ji87] C-R. Ji, A. Sill, and R. Lombard-Nelson, Phys. Rev. **D36**(1987) 165

[Ki87] I.D. King and C.T. Sachrajda, Nucl. Phys. **B279** (1987) 785

[Li92] H-N. Li, SUNY-Stony Brook report ITP-SB-92-25

[Li88] J. W. Lightbody and J. S. O'Connell, Computers in Physics, May/June (1988) 57

[Ra91] A.V. Radyushkin, Nucl. Phys. **A527**(1991) 53

[St91a] P. Stoler, V. Burkert, M. Tauiti, et al. CEBAF Experiment E-91-002, "The Study of Baryons at High Momentum Transfer with the CLAS Spectrometer"

[St91b] P. Stoler, Phys. Rev. Lett., **66** (1991) 1003;
P. Stoler, Phys. Rev. **D44** (1991) 73

[St93] P. Stoler, Physics Reports, **226** (1993) 103

[Wa90] G.A. Warren and C.E. Carlson, Phys. Rev. **D42** (1990) 3020

[Zh94] A. Zhitnitsky, Southern Methodist University, Preprint SMU-HEP-94-01

A Appendix. Relationship Between Multipoles and Measured Data

With unpolarized beam and target the double differential cross section for electrons and pions may be written

$$\frac{d\sigma}{d\Omega_e dE d\Omega_\pi} = \Gamma \frac{d\sigma}{d\Omega_\pi} \tag{3}$$

where $d\sigma/d\Omega_\pi$, the virtual photon cross section for pions emitted at angles (θ, ϕ) relative to the direction of the virtual photon, may be expressed as

$$\frac{d\sigma}{d\Omega_\pi} = F\{A(\theta) + \epsilon B(\theta) + \epsilon C(\theta)\cos(2\phi)\sin^2\theta + \sqrt{\epsilon(\epsilon+1)}D(\theta)\cos\phi\sin\theta\} \tag{4}$$

In eq. 3 Γ is the virtual photon flux factor

$$\Gamma = \frac{\alpha K}{2\pi^2 Q^2}\frac{E'}{E}\frac{1}{1-\epsilon},$$

$$F \equiv \frac{|\vec{p}_\pi|W}{MK},$$

and K is the equivalent real photon energy

$$K = \frac{W^2 - M_N^2}{2M_N}$$

Defining $\bar{A}_i \equiv A_i + \epsilon B_i$, the multipole decomposition of the coefficients up to a maximum $l = 1$ are (see [Do78]):

$$\begin{aligned}
\bar{A}_0 &= \{|E_{0+}|^2 + |M_{1-}|^2 + \tfrac{5}{2}|M_{1+}|^2 + \tfrac{9}{2}|E_{1+}|^2 - 3\,\mathrm{Re}(M_{1+}E_{1+}^*) \\
&\quad + \mathrm{Re}[(3E_{1+} + M_{1+})M_{1-}^*] \\
&\quad + \epsilon(|k^2|/|\mathbf{k}|^2)[|S_{0+}|^2 + |S_{1-}|^2 + 4|S_{1+}|^2 - 4\,\mathrm{Re}(S_{1+}S_{1-}^*)]\} \\
\bar{A}_1 &= \{2\,\mathrm{Re}[E_{0+}(3E_{1+} + M_{1+})^*] + \epsilon(|k^2|/|\mathbf{k}|^2)2\,\mathrm{Re}[S_{0+}(4S_{1+} + S_{1-})^*]\} \\
\bar{A}_2 &= \{-\tfrac{3}{2}|M_{1+}|^2 + \tfrac{9}{2}|E_{1+}|^2 + 9\,\mathrm{Re}(M_{1+}E_{1+}^*) - 3\,\mathrm{Re}[(3E_{1+} + M_{1+})M_{1-}^*] \\
&\quad + \epsilon(|k^2|/|\mathbf{k}|^2)[12|S_{1+}|^2 + 12\,\mathrm{Re}(S_{1+}S_{1-}^*)]\} \\
C_0 &= \{-\tfrac{3}{2}|M_{1+}|^2 + \tfrac{9}{2}|E_{1+}|^2 - 3\,\mathrm{Re}(M_{1+}E_{1+}^*) + 3\,\mathrm{Re}[(E_{1+} - M_{1+})M_{1-}^*]\} \\
D_0 &= -\{|k^2|/|\mathbf{k}|^2\}^{1/2}\,\mathrm{Re}[S_{0+}(3E_{1+} - M_{1+} + M_{1-})^* - E_{0+}(2S_{1+} - S_{1-})^*] \\
D_1 &= -6\{|k^2|/|\mathbf{k}|^2\}^{1/2}\,\mathrm{Re}[S_{1+}(E_{1+} - M_{1+} + M_{1-})^* + S_{1-}E_{1+}^*]
\end{aligned}$$

By retaining only M_{l+} and E_{l+}, and neglecting terms in $|E_{l+}|^2$ yields eqs. 2 in the text.